

Reviews

Mathematical modeling of heterogeneous catalytic reactions and processes

A. A. Samarskii and M. G. Slin'ko*

*Institute of Mathematical Modeling, Russian Academy of Sciences,
4a Miusskaya pl., 125047 Moscow, Russian Federation.
Fax: +7 (095) 972 0723*

The problems of heterogeneous catalysis are considered using mathematical modeling of catalytic reactions beginning from the atomic and molecular level. Some problems of the nonlinear dynamics of heterogeneous catalytic reactions are discussed. Mathematical models of these systems were designed using a combination of laboratory and computer experiments. The results of simulation of the nonlinear phenomena involved in the reactions $\text{NO} + \text{CO}$, $\text{NO} + \text{H}_2$, and $\text{CO} + \text{O}_2$, which are important for environmental catalysis, are discussed.

Key words: heterogeneous catalysis, mathematical modeling; bifurcation analysis, self-oscillations; chaos; autowaves.

Heterogeneous catalytic reactions and processes are based on a multilevel ordered structure. Three main levels can be distinguished: atomic and molecular microlevel (1–1000 Å), mesolevel (1–100 μm), and macrolevel (>100 μm). Depending on the purpose of the study and the characteristic structural features of a particular system, intermediate levels can also be distinguished. A level should be separated in such a way as to provide the possibility of its experimental investigation. The regularities of a process observed at a particular level should be independent of its scale. The influence of the scale should be determined by the initial and boundary conditions. The main interactions are those occurring between neighboring levels; however, the influence of higher levels also cannot be ruled out. Coordination, consistency, and integration of processes at different levels is significant. The atomic and molecular level is the most important for solving problems of catalysis. Processes occurring at this level determine the activity of catalysts and the reaction selectivity.

Nowadays, new procedures have been developed, which substantially extend the possibilities of investigation of catalysis at the molecular level and also allow investigation of the elementary steps of chemical transformations and of short-lived intermediate species.

New experimental and mathematical methods based on the use of computers are especially important at any investigation stage.

The purpose of the present paper is to survey the results of mathematical simulation of catalytic processes at the micro- and mesolevels.

The most notable achievements in modern physics and engineering have resulted from computer experiments.¹ Mathematical modeling based on a combination of computer and real experiments has triggered a new approach to the study of chemical systems and, in particular, catalysis.² This united the problems of chemical kinetics, air mechanics, physics, mathematics, and technology. Not only has the amount of the information gained changed but also the way of thinking in the study

of catalysis and understanding of the phenomena involved.

In our studies, mathematical models were developed based on the optimum and balanced relationship between the computer and real experiments and the fundamental laws of physics and chemistry. The balance between the computer and real experiments is one of the most difficult problems in research work.

Modeling of catalytic processes at the molecular level is needed to elucidate at the meso- and macroscopic levels the dependence of the chemical transformation rates on the composition of the reaction medium, the transfer coefficients and the properties of the reaction surface upon the degree of surface coverage with the reactants. Transition to microlevel models is also necessary in order to interpret the results of experimental studies and to determine the rate constants for the elementary steps and the model parameters.

The fullest mathematical model of a nonideal adsorbed surface layer is a distributed model taking into account the interactions of adsorbed particles, their mobility, and the possibility of order-disorder type surface rearrangements under the influence of adsorbed substances (phase structural transitions). The interatomic and intermolecular interactions of adsorbed particles and their state on the catalyst surface constitute the basis of all the elementary steps of a catalytic process; however, only a minor fraction of studies is aimed at investigating the interaction proper. Meanwhile, the significance and reliability of the results depend on the degree to which the assumed interatomic interaction potential is correct from the physicochemical viewpoint. The type and character of the interatomic forces between adsorbed species is the main point. Intermolecular forces are more diverse and, as a rule, anisotropic. At low coverages of adsorbed species, no surface structures are formed. When the number of adsorbed species and the rates of their surface migration increase, their interaction yielding polyatomic surface structures becomes more probable. As has been shown previously,³ these structures can be fairly stable and form islets of adsorbed species.

Polyatomic associates prove to be more stable. Thus, it can be concluded that the interatomic forces on a catalyst surface are essentially unpaired, *i.e.*, their interaction depends on the surrounding by other species. The theory of interatomic interactions on a catalyst surface has not been completed even in its fundamentals; no quantum-chemical approaches have been outlined yet. Only some mechanisms of the formation of interatomic forces are known. Presumably, the exchange interactions between two adsorbed species are characterized by important specific features. The exchange forces act at short distances and result in repulsion. The long-range dispersion forces are always attraction forces; therefore, in what follows we assumed repulsion between the first neighbors and attraction between the second neighbors. Taking into account the fundamental role of the interac-

tion parameters and the fact that at present they cannot be theoretically determined, we used the effective values of interaction parameters found using the whole set of available experimental data on adsorption, desorption, thermodesorption, and including analysis of thermo-reaction spectra, phenomena of hysteresis and self-oscillations of the reaction rate, as well as analysis of experimental data on adsorption layers obtained by various physicochemical methods used for surface studies.

A layer of adsorbed particles corresponds to the two-dimensional lattice-gas model, which is a typical model of statistical mechanics. At present, this model is widely employed to simulate elementary processes on a catalyst surface. The main parameters of this model are the energies of the lateral interaction of species located in various cells of the lattice. In the case of chemisorption of simple species, an adsorbed particle occupies one unit cell. A catalytic process consists of a combination of adsorption, desorption, and diffusion elementary steps and the elementary event of reaction, which are realized in a certain set of cells (points) of the lattice. The change in the state of the catalyst surface is described by the main kinetic equation:⁴

$$\begin{aligned} dP(\{A\})/dt = & P(\{A\}) \sum_{\{A\}} V(\{A\} \rightarrow \{A'\}) - \\ & - P(\{A'\}) \sum_{\{A'\}} V(\{A'\} \rightarrow \{A\}), \end{aligned} \quad (1)$$

where $P(\{A\})$ and $P(\{A'\})$ are states A and A' , respectively; V is the probability of transition from one state to the other. The transition from state A to state A' is determined by the change in the state of some point set of the fragment $\Omega(M, N)$.

The numerical solution of the main kinetic equation can be found using two different approaches: stochastic and deterministic. The stochastic approach is based on statistic testing (the dynamic Monte Carlo method). A drawback of this method is its substantial calculation cost; an advantage of this method is the possibility to precisely take into account the correlations in the arrangement of species on the catalyst surface. The deterministic approach is based on the solution of sets of linear differential equations. If lateral interactions are taken into account, these equations can be derived only using some approximations, for example, the quasichemical approximation. In this case, the models of the microscopic level consist of nonlinear ordinary differential Eq. (1) obtained by averaging the main equation

$$\begin{aligned} d\theta_{\alpha}^p/dt = F_{\alpha}^p, \quad d\theta_{\alpha\beta}^{pq}/dt = F_{\alpha\beta}^{pq}, \\ d\theta_{\alpha\beta\gamma}^{pqr}/dt = F_{\alpha\beta\gamma}^{pqr}, \end{aligned} \quad (2)$$

$$p, q, r = 1, 2, \dots, S - 1,$$

$$\alpha, \beta, \gamma \in \Omega(M, N),$$

where θ_{α}^p , $\theta_{\alpha\beta}^{pq}$, and $\theta_{\alpha\beta\gamma}^{pqr}$ are the probabilities of one-, two-, and three-point configurations.

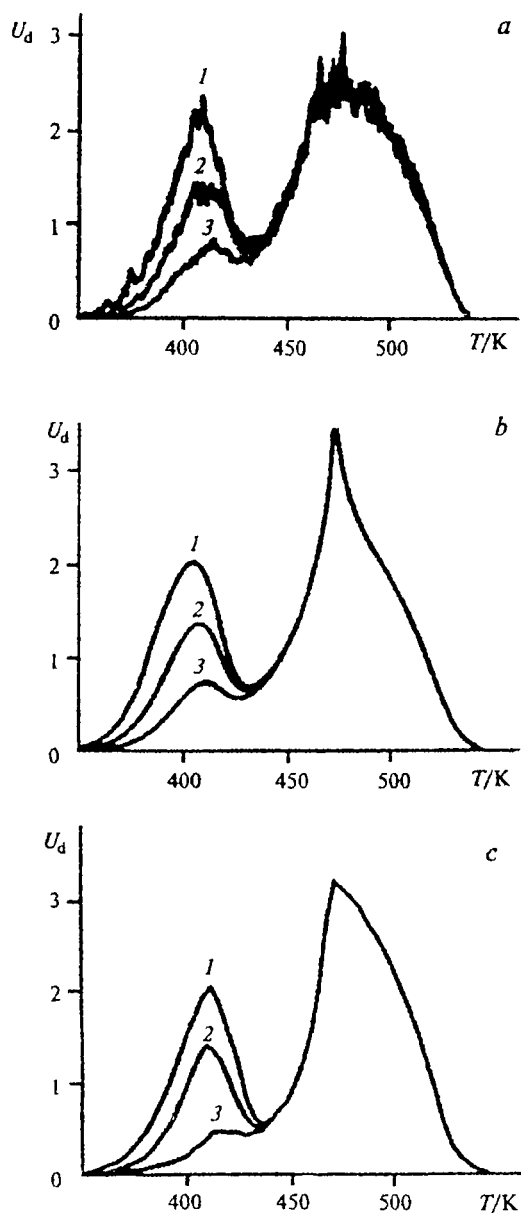


Fig. 1. Temperature dependences of the desorption rate (U_d) in the CO/Ru(001) system calculated using the Monte Carlo algorithm, stochastic model (a); calculated by integrating the equations of the deterministic model (b); measured experimentally (c). The thermal spectra correspond to different initial coverages $\theta_{\text{CO}}(0) = 0.49$ (1), 0.43 (2), and 0.38 (3).

As an example of using these approaches, we shall consider thermodesorption of CO molecules from the Ru(001) plane.⁵ The experimental thermodesorption spectra for several values of the initial surface coverage with adsorbed CO molecules are presented in Fig. 1, a. A significant feature of these spectra is the presence of several local maxima. The equation of ideal kinetics (3) does not take into account the lateral interaction and cannot explain the occurrence of two maxima in the

thermodesorption spectra at any values of the parameters.

$$d\theta_{\text{CO}}(t)/dt = -\nu \cdot \exp[-E/(RT)]\theta_{\text{CO}}, \quad (3)$$

$$T = T_0 + \beta t.$$

Here T is the temperature of the surface, β is the heating rate, and ν and E are the preexponent and the activation energy of desorption. The traditional quasichemical approximation gives correct results only when the interactions between the adsorbed particles are weak; when the interactions are strong, this approximation becomes too rough. In order to take into account the possibility of phase transitions in a substantially nonideal adsorbate layer, the quasichemical approximation can be made more general by introducing sublattices. The distributed mathematical model thus formed operates in terms of probabilities of filling $\theta_i(t)$ of points i of a fragment Ω in an ideal triangular lattice.

The monomolecular thermodesorption process is modeled by numerical solution of the Cauchy problem for the set of nonlinear ordinary differential equations:⁵

$$d\theta_{\text{CO}}(t)/dt = -R_{\text{des}} - \sum_j (R_{\text{mig},ij} - R_{\text{mig},ji}).$$

The first term corresponds to the rate of the variation of the probability θ_i as a result of elementary events of desorption. The sum determines the rate of variation of the probability θ_i upon the events of migration from a point i to neighboring point j and back. The rates of elementary events are calculated taking into account the lateral interactions of the first and second neighbors of adsorbed particles, described by energy parameters ε_1 and ε_2 , and also for the interactions of activated complexes with neighboring adsorbed particles.

Previously,⁵ the values of the parameters were fitted and a good mathematical description of the experimental thermodesorption spectra was obtained (see Fig. 1, b). The calculations were carried out for the $\Omega(3,3)$ fragment, which suffices for the description of a homogeneous surface coverage by the $(\sqrt{3} \times \sqrt{3})R30^\circ$ superstructure. Based on the selection of parameters providing satisfactory agreement between the results of calculations and the experimental thermodesorption spectra for the CO/Ru(0001) system, parameters of the lateral interactions between the adsorbed species were determined ($\varepsilon_1 \approx -1500 \text{ cal mol}^{-1}$ and $\varepsilon_2 \approx 500 \text{ cal mol}^{-1}$).

Stochastic modeling allows one not only to verify the results of deterministic calculations but also to "penetrate" into the microlevel, follow in detail the change in the adsorption layer, and comprehensively interpret the phenomena observed. In the calculations by the dynamic Monte Carlo method, thermodesorption is considered as a stochastic Markov process with a discrete set of states for a flow of elementary events (desorption and migration elementary events), which occur in a certain (sufficiently large) fragment of the surface lattice. The state of the fragment changes upon consecutive occur-

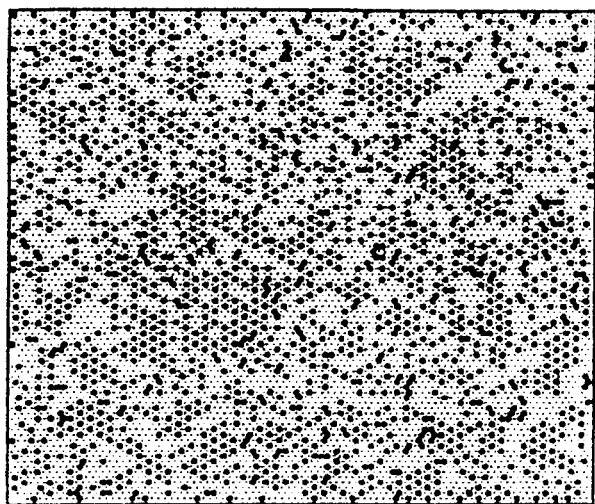


Fig. 2. Momentary picture of the state of a fragment of the Ru(001) surface lattice during thermodesorption of CO molecules at $T = 468$ K. The circles correspond to the adsorbed CO molecules, and dots correspond to vacant lattice points on the surface. The picture was obtained by Monte Carlo calculations

rence of elementary events. Figure 2 shows the momentary picture of the state of a lattice fragment at some time instant. It can be seen that during thermodesorption, some of the adsorbed species form the $(\sqrt{3} \times \sqrt{3})R30^\circ$ superstructure. This is due to the repulsion between the adsorbed CO molecules located at a distance corresponding to the first neighborhood and attraction between second neighbors. The high-temperature maximum of the thermodesorption spectrum is observed when the $(\sqrt{3} \times \sqrt{3})R30^\circ$ superstructure disappears and the surface coverage by CO molecules becomes low.

Comparison of the results obtained upon calculations by stochastic and deterministic models demonstrates that they agree with sufficient accuracy (see Fig. 1, b, c). Thus, the generalized quasichemical approximation makes it possible to calculate with high accuracy the rates of desorption even in the presence of strong interactions between the adsorbate species and under the conditions of formation of surface superstructures.

In the above-described case, we constructed a mathematical model, which fairly accurately takes into account the lateral interactions and reproduces the ordering processes in the adsorption layer. However, in the case of multistep reactions involving several types of adsorbed species, this detailed description results in unduly cumbersome equations. In some cases, complex reactions can be described in terms of less detailed models. It is significant that lateral interactions not only lead to ordering processes but also exert a considerable influence on the rates of elementary steps. This influence is present as well in the case of disordered (random) arrangement of the species on the surface.

The assumption of complete mixing allows considering complex reactions in terms of fairly simple models, which, nevertheless, do take into account the lateral interactions in the adsorbed layer. A model of this type provided an adequate mathematical description of various experimental data on the reaction $\text{NO} + \text{CO}/\text{Pt}(100)$.⁵⁻⁸

The reaction $\text{NO} + \text{CO} \rightarrow \text{CO}_2 + 1/2 \text{N}_2$ is important from the viewpoint of environment protecting catalysis, because the initial reactants are toxic components of exhaust gases from internal combustion engines. The development of efficient afterburners for exhaust gases seems possible only with a deep insight into the physicochemical processes that occur at the gas-catalyst interface.

In addition, the reaction $\text{NO} + \text{CO}/\text{Pt}(100)$ demonstrates a complex dynamic behavior. A number of interesting phenomena have been discovered, for example, multiplicity of steady states, surface explosion, and self-oscillations of the reaction rate.^{6,7}

The reaction $\text{NO} + \text{CO}/\text{Pt}(100)$ is studied theoretically within the framework of the kinetic scheme comprising nine elementary steps:⁵

- | | |
|---|----------------------------|
| 1) $(\text{NO})_{\text{gas}} + * \rightarrow (\text{NO})_{\text{ads}}$ | NO adsorption, |
| 2) $(\text{CO})_{\text{gas}} + * \rightarrow (\text{CO})_{\text{ads}}$ | CO adsorption, |
| 3) $(\text{NO})_{\text{ads}} \rightarrow (\text{NO})_{\text{gas}} + *$ | NO desorption, |
| 4) $(\text{CO})_{\text{ads}} \rightarrow (\text{CO})_{\text{gas}} + *$ | CO desorption, |
| 5) $(\text{NO})_{\text{ads}} + * \rightarrow (\text{N})_{\text{ads}} + (\text{O})_{\text{gas}}$ | NO dissociation, |
| 6) $(\text{CO})_{\text{ads}} + (\text{O})_{\text{ads}} \rightarrow (\text{CO}_2)_{\text{gas}} + 2*$ | CO ₂ formation, |
| 7) $(\text{O})_{\text{ads}} + (\text{O})_{\text{ads}} \rightarrow (\text{O}_2)_{\text{gas}} + 2*$ | O ₂ desorption, |
| 8) $(\text{N})_{\text{ads}} + (\text{N})_{\text{ads}} \rightarrow (\text{N}_2)_{\text{gas}} + 2*$ | N ₂ desorption, |
| 9) $(\text{N})_{\text{ads}} + (\text{O})_{\text{ads}} \rightarrow (\text{NO})_{\text{ads}} + *$ | NO formation. |

Here "*" is a free adsorption site; $(\text{NO})_{\text{ads}}$, $(\text{CO})_{\text{ads}}$, $(\text{N})_{\text{ads}}$, and $(\text{O})_{\text{ads}}$ are adsorbed species; and $(\text{NO})_{\text{gas}}$, $(\text{CO})_{\text{gas}}$, $(\text{N}_2)_{\text{gas}}$, $(\text{O}_2)_{\text{gas}}$, and $(\text{CO}_2)_{\text{gas}}$ are molecules in the gas phase. The $(\text{N}_2)_{\text{gas}}$, $(\text{CO}_2)_{\text{gas}}$, and $(\text{O}_2)_{\text{gas}}$ molecules formed in the reaction.

The discovery of oscillations and hysteresis in the $\text{NO} + \text{CO}/\text{Pt}(100)$ reaction indicates that ordinary equations of ideal kinetics cannot provide an adequate mathematical description of this process. Previously, it has been shown⁵ that the complex behavior of the $\text{NO} + \text{CO}/\text{Pt}(100)$ system is mainly due to lateral interactions in the adsorbate layer. These interactions cause significant nonlinearity of the kinetic equations. To model the $\text{NO} + \text{CO}$ reaction on the Pt(100) plane in the (1×1) phase, a lumped four-component model has been proposed; this model describes the system dynamics in terms of the densities of coverage of the catalyst surface by carbon monoxide (θ_{CO}) and nitrogen monoxide (θ_{NO}) molecules and oxygen (θ_{O}) and nitrogen (θ_{N}) atoms.⁶ A significant feature of this model is that it takes into account the lateral interactions and can be strictly derived from the main kinetic equation provided that the adsorbed layer is disordered. The mathematical model is based on a set of four nonlinear ordinary differential equations.

The model parameters were selected by a step-by-step procedure based on experimental data for processes containing only one or several steps from the general kinetic scheme. In particular, mathematical modeling for the thermoreaction and thermodesorption processes involving preadsorbed NO and CO molecules was carried out. Experimental studies showed that these processes are quite unusual.⁸ If at the initial time instant only NO molecules are present on the surface, they dissociate and the resulting N₂ molecules are slowly desorbed over a wide temperature range (Fig. 3, a). In the case where CO molecules are also present, a very narrow peak appears in the low-temperature region of the CO₂ thermodesorption spectrum (see Fig. 3, b). This effect is referred to as "surface explosion". A similar narrow peak occurs in the N₂ thermodesorption spectrum. If $\theta_{\text{CO}}(0) > \theta_{\text{NO}}(0)$, then nitrogen is completely desorbed during the "surface explosion". Thus, it turns out that in the presence of CO molecules, dissociation of NO occurs very rapidly, whereas in the absence of CO, it occurs slowly. The models proposed previously⁸ did not describe this set of experimental findings. The results of subsequent modeling⁶ demonstrated that an adequate theoretical description of the above-listed facts can be obtained by taking into account the step of NO

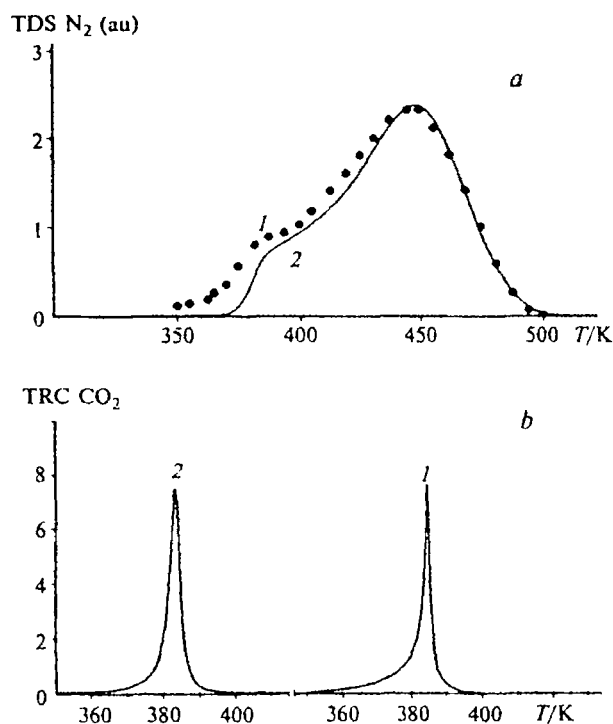


Fig. 3. Experimental (1) and calculated thermal (2) spectra of N₂ and CO₂ in the NO + CO/Pt(100) system: (a) thermodesorption spectra (TDS) obtained for the initial coverages $\theta_{\text{NO}}(0) = 0.25$, $\theta_{\text{CO}}(0) = 0$, $p = 2 \text{ K s}^{-1}$; dots correspond to experimental results, and the line corresponds to the model; (b) thermoreaction spectra (TRS) obtained for $\theta_{\text{NO}}(0) = \theta_{\text{CO}}(0) = 0.2$, $U_{\text{CO}_2} \times 100$.

formation (step 9), which had not been supposed previously.

A distinctive feature of the system under study is the kinetic rate self-oscillations, which have an "explosive" character.⁷ The model developed also allows the existence of periodic solutions corresponding to the self-oscillations of the reaction rate and substantiates their appearance. An important role in the mechanism of oscillations is played by lateral interactions. To describe this mechanism, we shall divide a single cycle of self-oscillations into three main stages (Fig. 4).

I. The coverage of the surface by NO and CO molecules. During the first stage, the surface is rapidly covered mostly with NO molecules, because the NO partial pressure p_{NO} is higher than p_{CO} . As this takes place, the dissociation of NO slows down, because it is hampered by the neighboring adsorbed NO molecules. Since the number of adsorbed oxygen atoms is low, the rates of CO₂ formation remain low.

II. The displacement of the NO molecules by adsorbed CO molecules. During this stage, the concentration of adsorbed CO molecules increases, while that of adsorbed NO species decreases. The rates of formation of CO₂ remain virtually unchanged. The NO molecules are displaced as a result of the corresponding influence of adsorbed CO molecules on the NO desorption rates, which is due to the repulsive interactions between these molecules.

III. "Surface explosion." When the surface concentration of NO molecules becomes sufficiently low, the rates of NO dissociation start to increase, and autocata-

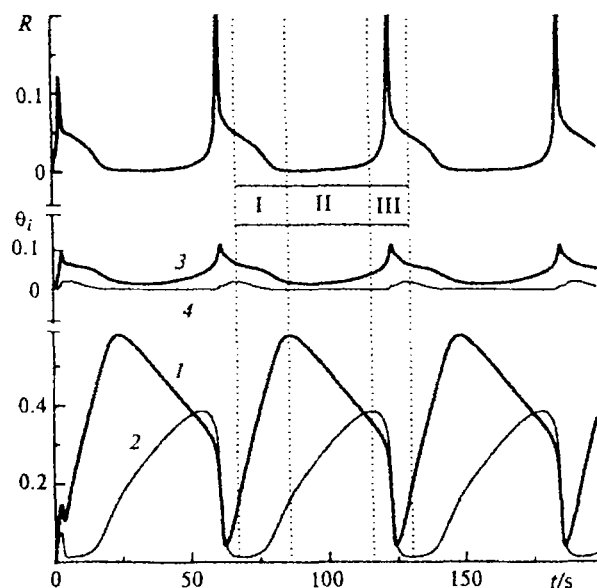


Fig. 4. Kinetic oscillations of the reaction rate (R) and surface coverages (θ_i) with NO (1), CO (2), N (3), and O (4) in the four-component model for the NO + CO/Pt(100) reaction at $p_{\text{CO}} = 3.0 \cdot 10^{-7} \text{ Mbar}$, $p_{\text{NO}} = 4.8 \cdot 10^{-7} \text{ Mbar}$ and $T = 390 \text{ K}$. To discuss the mechanism of oscillations, one cycle was divided into three stages (I—III).

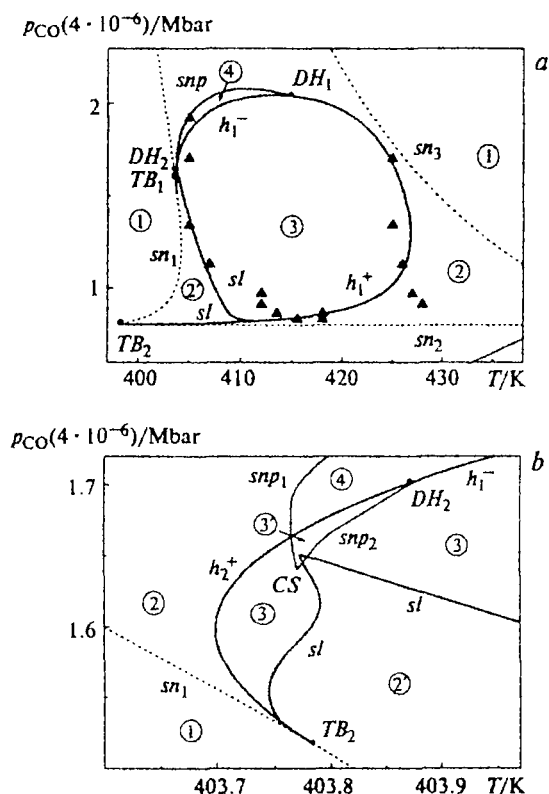


Fig. 5. *a*, Bifurcation diagram on a plane ($p_{\text{CO}} = 4 \cdot 10^{-6}$, T) at a constant pressure, $p_{\text{NO}} = 5 \cdot 10^{-6}$ Mbar. *b*, Section of the bifurcation diagram located near points TB_1 and DH_2 (shown on an enlarged scale).

Lines of co-dimension 1 bifurcations: sn is a twofold equilibrium; h^+ is the Andronov—Hopf line (supercritical); h^- is the Andronov—Hopf line (subcritical); sl is the separatrix loop; snp is a double cycle. Co-dimension 2 bifurcations: TB is the Tackens—Bogdanov line ($sn/h^+/h^-$); DH is zero of the first Lyapunov value ($snp/h^+/h^-$). Regions (1)—(4) are characterized by qualitatively different phase space "portraits" and correspond to different dynamic behavior of the system: 1, single-steady-state region; 2, 2', regions of three steady states;⁹ 3, oscillations; 4, three steady states plus two limit cycles, stable and unstable. Triangles mark the experimental data determining the range of self-oscillations.

lytic increase in the reaction rate is observed. As a result, the adsorption layer is rapidly removed, the state of the surface becomes the same as it has been in the beginning of the first stage, and the whole cycle is repeated once again.

Previously,⁹ a detailed bifurcation analysis of the proposed model has been carried out, and bifurcation diagrams based on a large number of external parameters have been constructed. An example of this type of diagram is shown in Fig. 5. The bifurcation analysis of stationary and periodic solutions made it possible to identify precisely the regions characterized by qualitatively different dynamic behavior of the system. The

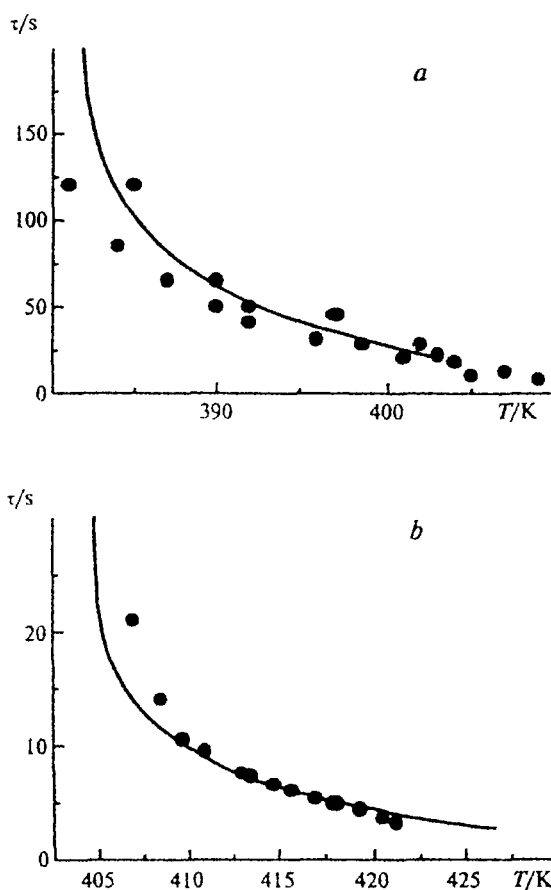


Fig. 6. Comparison of the calculated and experimental temperature dependences of the self-oscillation period (τ) in the $\text{NO} + \text{CO}/\text{Pt}(100)$ system for two sets of external parameters: *a*, $p_{\text{NO}} = 4.8 \cdot 10^{-7}$ Mbar, $p_{\text{CO}} = 3.0 \cdot 10^{-7}$ Mbar; *b*, $p_{\text{NO}} = 5.0 \cdot 10^{-6}$ Mbar, $p_{\text{CO}} = 2.8 \cdot 10^{-6}$ Mbar. Dots show the experimental results and the line corresponds to the model.

region of existence of self-oscillations is confined by the Andronov—Hopf bifurcation line h_1^* (on the right in the diagram), the line sl of the saddle separatrix loop, and the line snp of multiple cycles. Figure 5 also shows the experimental data that determined the region of self-oscillations. The figure demonstrates good agreement of the boundaries of the self-oscillation region built using the mathematical model with those found experimentally.

The designed model provides a fairly accurate description of the experimental data on the temperature dependence of the period of self-oscillations (Fig. 6). At relatively high temperatures, self-oscillations arise in a soft regime as a result of the supercritical Andronov—Hopf bifurcation. As the temperature decreases, the period and amplitude of the self-oscillations increase monotonically. At low temperatures, the surface is covered with CO molecules, and a state characterized by low rates is established in the system. The limit cycle

corresponding to the self-oscillation regime transforms into the saddle separatrix loop.

In a previous study,¹⁰ mathematical modeling of the nonlinear phenomena involved in the reaction between NO and H₂ at the Rh(111) plane was carried out. A mathematical model was constructed; the model consisted of five ordinary differential equations describing the change in the concentrations of adsorbed species on the catalyst surface and took into account the lateral interactions in the adsorption layer. The parameters of lateral interactions were determined using analysis of thermodesorption and thermoreaction spectra known for this system.^{10,11} The results of the mathematical modeling made it possible to elucidate the origin for the experimentally observed self-oscillations of the reaction rate and the hysteresis in the variation of the reaction rate as a function of temperature and hydrogen pressure. It was found that lateral interactions in the absorption layer are the main reason for the complex dynamic behavior of the NO + H₂/Rh(111) reaction. The reaction rate self-oscillations are accompanied by autocatalytic accumulation of the intermediate compound NH on the catalyst surface. Owing to the definite character of the lateral interactions occurring in this system, accumulation of NH decreases the rates of hydrogen desorption and NO dissociation. As a result of this process, the concentration of hydrogen atoms on the surface decreases, and the NH species accumulated by this time start to decompose. The decrease in the NH concentration results, in turn, in the acceleration of hydrogen adsorption and NO dissociation. Consequently, the reaction rates increase, and the concentration of adsorbed nitrogen atoms increases. The simultaneous increase in the concentrations of adsorbed N and H atoms results in autocatalytic formation of NH on the Rh(111) surface, and the oscillation cycle is thus closed.

The point model designed in a previous study¹⁰ was used to develop a distributed model of the reaction-diffusion type aimed at describing the dissipative structures formed on the surface of the Rh(111) single crystal plane during the NO + H₂ reaction.¹² In an experimental study of this reaction by photoelectron emission spectroscopy (PEEM), travelling pulses and spiral waves were detected on the catalyst surface.¹³ The phenomenon of distance interaction of two moving autowaves unknown previously was also discovered. This phenomenon consists in the formation of bright areas with low work function when two running pulses approach each other. To describe the spatial structures detected experimentally, a mathematical model for the NO + H₂/Rh(111) reaction was constructed with allowance for the diffusion of adsorbed species (NO, H, O, N, NH) over the catalyst surface. The model comprises a set of five partial differential equations. The numerical integration of the reaction-diffusion type equations in one- and two-dimensional regions made it possible to describe in detail the reasons for the generation of the autowave processes observed experimentally during the

reaction. In addition, the results of the computer experiment made possible predicting the formation of stationary localized structures that had not been detected in the laboratory experiment. During the numerical modeling, some spatiotemporal self-organization phenomena, such as chaotic spatiotemporal oscillations of localized structures and the "soliton-like" behavior of travelling pulses, were found for the first time.

The problem of the reasons for the generation of chaotic oscillations in heterogeneous catalytic systems presents considerable interest. No realistic mathematical models involving chaotic oscillations have existed up to now. The results of mathematical modeling presented in the study cited above¹² demonstrated the possibility of existence of spatiotemporal chaos, which, however, was not observed experimentally. Low-dimensional, temporal chaos was obtained in the mathematical modeling of the reaction between NO and H₂ at the Pt(100) face.¹⁴ In this system, transition to chaos according to the Feigenbaum scenario was detected experimentally in a very narrow range of hydrogen pressure in the initial mixture during its decrease. The calculated fractal dimension of the strange attractor constructed from experimental data was to 2.6, which indicates that it is possible to observe temporal chaos with a low dimension. To describe the experimental data obtained, a point mathematical model consisting of five ordinary differential equations and taking into account lateral interactions in the adsorbed layer was developed. The parameters of lateral interactions were determined using the analysis of thermodesorption and thermoreaction spectra known for this system. The chaotic oscillations in the model were found for the same temperatures and NO pressures as were observed in the experiment. Figure 7 shows the transition to chaos *via* a sequence of bifurcations doubling the period which was obtained in a numerical experiment upon a decrease in the hydrogen pressure in the initial mixture.

Complex dynamic regimes including deterministic chaos are also observed at higher levels. To model them, information obtained during mathematical modeling of the dynamic behavior at a lower level is required. An example of such a study is mathematical modeling of the chaotic rate oscillations in the oxidation of carbon monoxide on the Pd-zeolite catalyst.¹⁵

Experimental study of the CO oxidation on the Pd-zeolite catalyst revealed the complex character of the reaction rate oscillations.¹⁶ Depending on the experimental conditions, both regular and chaotic oscillations were observed. The Pd-zeolite catalyst consists of zeolite crystallites with inserted Pd clusters of virtually identical sizes (~10 nm). An interesting feature of the system under study is the fact that the character and properties of the observed oscillations depend substantially on the size of the zeolite crystallites. Thus, when the size of crystallites was 50 μm, complex irregular oscillations were observed. When the size was 5–7 μm, regular periodic oscillations were observed at low con-

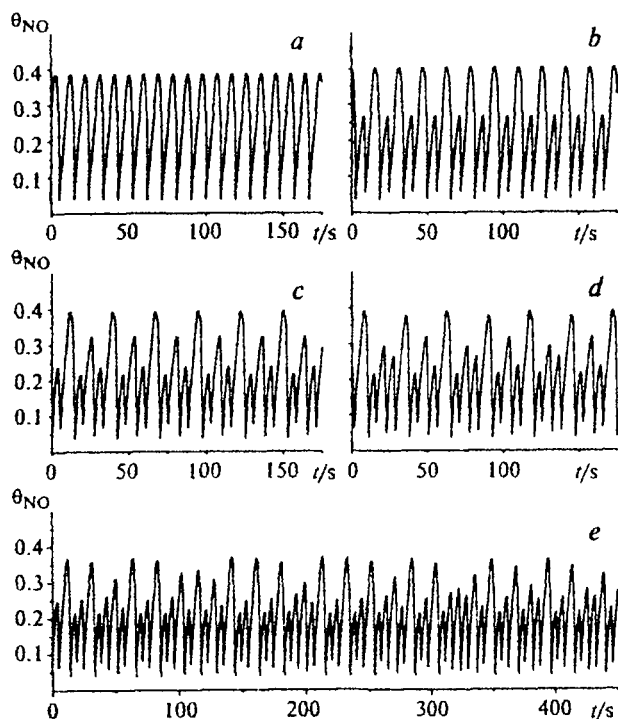


Fig. 7. Transition to chaos via a sequence of bifurcations of the period doubling, found in a numerical experiment upon a decrease in the hydrogen pressure in the initial mixture at $T = 457$ K and $p_{\text{NO}} = 5 \cdot 10^{-6}$ Mbar. *a*, periodic oscillations, $p_{\text{H}_2}/p_{\text{NO}} = 2.52$; *b*, oscillations with the 2-period, $p_{\text{H}_2}/p_{\text{NO}} = 2.50$; *c*, oscillations with the 4-period, $p_{\text{H}_2}/p_{\text{NO}} = 2.46$; *d*, oscillations with the 8-period, $p_{\text{H}_2}/p_{\text{NO}} = 2.4585$; *e*, deterministic chaos, $p_{\text{H}_2}/p_{\text{NO}} = 2.45$.

centrations of CO. As the concentration of CO increased, the system passed to chaotic oscillations. It has been suggested previously¹⁷ that complication of the pattern of oscillations and appearance of chaos are associated with the appearance of nonuniform CO concentrations within the bulk of the zeolite crystallite and with the influence of internal diffusion of CO on the reaction rates. In this case, the frequencies of the self-oscillations of the reaction rate on the surface of the Pd clusters located at different distances from the crystallite center can differ considerably. In this system, individual Pd clusters can be considered as local oscillators coupled to one another only through the gas phase, because diffusion of the reactant over the zeolite matrix is insignificant. Thus, it has been suggested that the nonuniformity of the CO concentration in a zeolite crystallite might account for the breakdown of the synchronization of the local oscillators and lead to a chaotic regime.

To verify this hypothesis, a mathematical model of the oxidation of CO on the Pd-zeolite catalyst that took account of the internal diffusion of CO in the zeolite

matrix has been designed.¹⁵ The zeolite catalyst was assumed to consist of a large number of identical crystallites of the spherical shape. It was also assumed that all the Pd clusters are identical and are uniformly distributed over the crystallite bulk. To take into account the internal diffusion of the gas, the crystallite was divided into N spherical layers with equal volumes. Since the pressure of oxygen was two orders of magnitude higher than the pressure of carbon monoxide, the former was considered to be constant and only variation of the CO pressure in the crystallite bulk was taken into account. The CO pressure in each layer was taken to be constant and the palladium clusters were considered to be identical. The model was designed based on the weight balance of the gas in each layer of the zeolite crystallite as a result of diffusion and the reaction.

$$\begin{aligned} dp_n/dt = D[d_{n-1}(p_{n-1} - p_n) + d_n(p_{n+1} - p_n)] - \\ - \sigma G(X_n, p_n), \quad dX_n/dt = F(X_n, p_n), \quad (4) \\ 1 \leq n \leq N, p_0 = 0, p_{N+1} = p_{\text{CO}}. \end{aligned}$$

This system can be considered as a chain of parametrically related chemical oscillators. The first equation establishes the relationship between the neighboring oscillators resulting from diffusion of CO in the crystallite. The first two terms on the right-hand side of this equation are a discrete analog of the diffusion operator. The third term is equal to the amount of CO, consumed due to the reaction in an i th layer. Each i th oscillator is described by a point model for the oxidation of CO on the surface of Pd clusters located in one spherical layer of the crystallite. This model is a model of a lower level built using the data obtained in a study of the oxidation of CO on the Pd(110) single crystal plane. It consists of three equations describing the variation of adsorbed CO and O on the surface of the Pd cluster and the dissolved oxygen in the subsurface layer of the catalyst. The parameter p_i (the pressure of CO in an i th layer) determines the natural frequency of the oscillator. The strength of coupling between the oscillators depends on the ratio of the diffusion rate to the reaction rate. The slower the diffusion and the larger the amount of CO consumed in an i th layer, determined by the $G(p_i)$ function, the more "sensitive" the oscillators to one another, *i.e.*, the stronger the coupling. Chaotic oscillations were obtained at a substantial nonuniformity of the CO concentration over the radius of a zeolite crystallite in the region of the highest sensitivity of the dynamic behavior of external spherical layers to the variation of the CO pressure. Figure 8 shows the chaotic oscillations of the global reaction rate at $p_{\text{CO}} = 2.64$ Torr and a diffusion coefficient of 10^{-7} cm² s⁻¹ in the presence of excess oxygen for forty coupled oscillators.

Various dynamic regimes can also arise in catalytic reactors. For example, in the simplest object invariant with respect to the scale, *viz.*, in an ideal-mixing flow reactor, in which a first-order reaction occurs, multiple

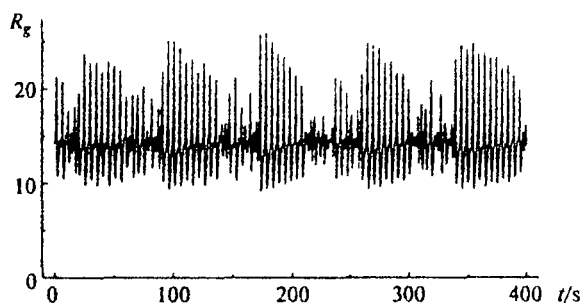


Fig. 8. Chaotic oscillations of the global reaction rate (R_g) obtained for a set of forty coupled oscillators at $p_{CO} = 2.64$ Torr, diffusion coefficient 10^{-7} cm² s⁻¹ in excess oxygen.

steady states and oscillation regimes are possible. The mathematical model for this reactor has the following form:¹⁸

$$\begin{aligned} dx/dt &= -x + f, \\ 1/B \cdot d\theta/dt &= -g\theta + f, \\ f &= k \cdot \exp[\theta/(1 + \beta\theta)] \cdot (1 - x), \\ B &= \Delta\theta_{ad}/(1 + (V_c/W)/(c_c/c_r)), \end{aligned} \quad (5)$$

where x is the degree of conversion, $\theta = E(T - T_0)/RT_0^2$ is temperature; k is the rate constant for the reaction; $g = (1 + \gamma)/\Delta\theta_{ad}$ is the heat removal parameter; $\Delta\theta_{ad}$ is the adiabatic heating, $g = \alpha F/Wc_r$, $\beta = RT/E$; α is the heat transfer coefficient, F is the cooling surface area; W and c_r are the volume and the heat capacity of the reaction mixture; and V_c and c_c are the volume and the heat capacity of the catalyst; all the parameters of Eq. (5) are nondimensional.¹⁹

The diversity of the phase portraits possible in terms of model (5) has been demonstrated in numerous works. Thus in a study,²⁰ only nine phase portraits containing stable and unstable steady states of the type of nodes or focuses and also stable and unstable limiting cycles were found; however, a more comprehensive analysis carried out later²¹ has shown that 35 phase portraits exist and that 31 of them are characterized by multiplicity of steady states. An even more detailed bifurcation analysis¹⁹ revealed 51 phase portraits. In this work, the ranges of parameters, in which up to three limiting cycles exist near the high-temperature regime, were identified. In an ideal-mixing reactor, chaotic regimes are possible only in the case where the temperature of the cooling agent changes periodically with a relatively large amplitude or when a reaction of the $A \rightarrow B \rightarrow C$ type occurs.

The studies considered above indicate that substantial experience of the mathematical modeling of catalytic systems at various levels, starting from the molecular level, has been accumulated by now. Based on

distributed mathematical models of micro- and meso-levels, the self-organization phenomenon and the appearance of chaotic regimes (chemical turbulence) have been investigated; the dynamics of phase transitions has been studied.

Thus, mathematical models of heterogeneous catalytic systems, starting from the molecular level, are distributed, nonlinear, multiparametric, and multidimensional and are based on multiparticle interactions of the adsorbed species, their mobility, and surface nonuniformity. The multiplicity of the steady states, their stability, the appearance of ordering of adsorbed species, and the reconstruction of the catalyst surface under the action of adsorbed species depend on the surface coverages.

The instability of steady states is an important feature of heterogeneous catalytic systems. The instability and nonlinearity result in self-oscillations of the reaction rate, autowaves of various types, ordered structures, and chaotic regimes (chemical turbulence) at any scale level of catalytic systems. The evolution of a catalytic system includes consecutive events of replacement of a stable state by another one, which pass through unstable states, as well as phase transitions of the order-disorder and phase separation types. The kinetics of heterogeneous reactions is determined by the state of the surface at the molecular level. To determine the rates of elementary steps and the critical conditions, it is necessary to use distributed nonlinear models based on cooperative interaction and mobility of adsorbed species. The model parameters (diffusion coefficients, sticking coefficients, and activation energy) depend on the surface coverages due to the influence of lateral interactions and phase transitions. Real reaction systems are nonuniform, owing to the spatiotemporal self-organization, and are described by distributed mathematical models.

The authors wish to thank A. G. Makeev, E. S. Kurkina, N. V. Peskov, G. G. Elenin, N. L. Semendyaeva, and M. M. Slin'ko (the laboratory of mathematical modeling in physics at the Department of Computation Mechanics and Cybernetics of the Moscow State University) for performing the works and to A. G. Makeev, E. S. Kurkina, and M. M. Slin'ko for preparation of the paper.

This work was financially supported by the Russian Foundation for Basic Research (Project No. 97-03-32232a).

References

1. A. A. Samarskii, *Vestn. Akad. Nauk SSSR [Bull. Acad. Sci. USSR]*, 1979, 38 (in Russian).
2. M. G. Slin'ko, *Plenary Lectures at the Conference on Chemical Reactions "Khimreaktor-1 - Khimreaktor XIII"* [Plenary Lectures at the Conference on Chemical Reactions "Khimreaktor-1 - Khimreaktor XIII"], Institute of Catalysis of the Siberian Branch of the RAS, Novosibirsk, 1996 (in Russian).

3. G. G. Elenin and A. G. Makeev, *Matem. modelirovanie [Mathematical Modeling]*, 1991, 29 (in Russian).
4. *Monte Carlo Methods in Statistical Physics*, Ed. K. Binder, Mir, Moscow, 1982, 400 pp.
5. A. G. Makeev and N. L. Semendyaeva, *Matem. modelirovanie [Mathematical Modeling]*, 1995, 29 (in Russian).
6. A. G. Makeev, *Matem. modelirovanie [Mathematical Modeling]*, 1996, 115 (in Russian).
7. T. Fink, J.-P. Dath, R. Imbihl, and G. Ertl, *J. Chem. Phys.*, 1991, **95**, 2109.
8. T. Fink, J.-P. Dath, M. R. Basset, R. Imbihl, and G. Ertl, *Surf. Sci.*, 1991, **245**, 96.
9. E. S. Kurkina and A. G. Makeev, in *VMK MGU [Department of Computation Mechanics and Cybernetics, Moscow State University]*, Moscow State Univ., Moscow, 1997 (in Russian).
10. A. G. Makeev, M. M. Slinko, N. M. H. Janssen, P. D. Cobden, and B. E. Nieuwenhuys, *J. Chem. Phys.*, 1996, **105**, 7210.
11. A. G. Makeev and M. M. Slinko, *Surf. Sci.*, 1996, **359**, L467.
12. A. G. Makeev, N. M. H. Janssen, P. D. Cobden, M. M. Slinko, and B. E. Nieuwenhuys, *J. Chem. Phys.*, 1997, **107**, 965.
13. N. M. H. Janssen, A. Schaaf, B. E. Nieuwenhuys, and R. Imbihl, *Surf. Sci.*, 1996, **364**, L555.
14. A. G. Makeev and B. E. Nieuwenhuys, *J. Chem. Phys.*, 1998, **108**, 3740.
15. E. S. Kurkina, N. V. Peskov, M. M. Slin'ko, and M. G. Slin'ko, *Dokl. Akad. Nauk*, 1996, **351**, 497 [*Dokl. Chem.*, 1996 (Engl. Transl.)].
16. M. M. Slin'ko, N. I. Jaeger, and P. Svensson, *J. Catal.*, 1989, **118**, 349.
17. M. M. Slin'ko, N. I. Jaeger, and P. Svensson, in *Proc. of the International "Conference Unsteady State Processes in Catalysis"*, Ed. Yu. Matros, Utrecht, 1990, 415.
18. V. S. Sheplev, *Modelirovanie kataliticheskikh reaktorov [Modeling of Chemical Reactions]*, Novosibirsk State Univ., Novosibirsk, 1987, 80 (in Russian).
19. V. S. Sheplev and M. G. Slin'ko, *Dokl. Akad. Nauk*, 1997, **352**, 781 [*Dokl. Chem.*, 1997 (Engl. Transl.)].
20. A. B. Poore, *Arch. Rat. Mech. Anal.*, 1973, **52**, 358.
21. D. A. Vaganov, V. G. Abramov, and N. G. Samoilov, *Dokl. Akad. Nauk SSSR*, 1977, **234**, 640 [*Dokl. Chem.*, 1977 (Engl. Transl.)].

*Received November 12, 1997;
in revised form February 3, 1998*